Unclassified
SECURITY CLASSIFICATION OF THIS PAGE

DTIC FILE COPY

REPORT DOCUMENTATION PAGE

Form Approved OMB No. 0704-0188

1a. REPORT SECURITY CLASSIFICATION: Unclassified	1b. RESTRICTIVE MARKINGS
AD-A200 376	
2a. SECURITY CLASSIFICATION AUTHORITY	3. DISTRIBUTION/AVAILABILITY OF REPORT: Approved for public release; distribution unlimited. (2)
2b. DECLASSIFICATION/DOWNGRADING SCHEDULE: OCT 1 3 1988 S D	
4. PERFORMING ORGANIZATION REPORT NUMBER(S): R910023-1	5. MONITORING ORGANIZATION REPORT NUMBER(S): AFOSR-TR- 88-1088
6a. NAME OF PERFORMING ORGANIZATION: Scientific Research Associates	6b. OFFICE SYMBOL (If applicable): 8N189
6c. ADDRESS (City, State, and ZIP Code): 50 Nye Road, Glastonbury, CT 06033	7a. NAME OF MONITORING ORGANIZATION: AFOSR
	7b. ADDRESS (City, State, and ZIP Code): Bldg 410, Bolling AFB DC 20332
8a. NAME OF FUNDING/SPONSORING ORGANIZATION: Air Force Office of Scientific Research	8b. OFFICE SYMBOL (If applicable): ~~NP~~ NE
8c. ADDRESS (City, State, and ZIP Code): Bolling Air Force Base, Washington, D.C. 20332	9. PROCUREMENT INSTRUMENT IDENTIFICATION NUMBER: F49620-87-C-0055
	10. SOURCE OF FUNDING NUMBERS: PROGRAM ELEMENT NO. 61102F; PROJECT NO. 2306; TASK NO B1; WORK UNIT ACCESSION NO.

11. TITLE (Include Security Classification)

Studying Quantum Phase-Based Electronic Devices

12. PERSONAL AUTHOR(S)
H. L. Grubin and J. P. Kreskovsky

13a. TYPE OF REPORT	13b. TIME COVERED	14. DATE OF REPORT (Year, Month, Day)	15. PAGE COUNT
Annual	FROM 871001 TO 880715	1988 September 01	17

16. SUPPLEMENTARY NOTATION

17. COSATI CODES			18. SUBJECT TERMS (Continue on reverse if necessary and identify by block number)
FIELD	GROUP	SUB-GROUP	
			Quantum Potential, Density Matrix, Resonant Tunnelling

19. ABSTRACT (Continue on reverse if necessary and identify by block number)

This report summarizes work performed during the reporting period 01 October 1987 to 15 July 1988 under Contract #F49620-87-C-0055. Work was confined to use of the moments of the density matrix, for examining transport in quantum phase based devices. There are two significant features of the approach: (1) the introduction of Bohm's quantum potential, and (2) the use of moment equations which are self-consistently coupled to Poisson's equation. There were a number of significant approximations made during this reporting period that are currently being eliminated: (1) Only two of the minimum of three moment equations have been implemented. (2) Boltzmann statistics was invoked. The results show for a double barrier structure with 500 Angstrom spacer-layers considerable structure in the charge distribution. At low values of bias and corresponding low values of current there is a buildup of charge upstream of the first barrier. As well as tunnelling into the well. At a critical value of bias a local instability of current occurs and the solutions shows a qualitative difference. Accumulation at the upstream barrier is only marginally altered, and there is a significant charge buildup in the well. The instability appears to be a precursor for this large charge buildup.

20. DISTRIBUTION/AVAILABILITY OF ABSTRACT	21. ABSTRACT SECURITY CLASSIFICATION
☐ UNCLASSIFIED/UNLIMITED ☐ SAME AS RPT. ☐ DTIC USERS	Unclassified
22a. NAME OF RESPONSIBLE INDIVIDUAL: Captain Kevin Malloy	22b. TELEPHONE (Include Area Code): (202) 767-4931 — 22c. OFFICE SYMBOL: NE

DD Form 1473, JUN 86 — Previous editions are obsolete.

SECURITY CLASSIFICATION OF THIS PAGE

Unclassified

19. Switching calculations were also performed and indicate switching times of the order of 200 femoseconds.

Contract No. : F49620-87-C-0055
SRA No. : R87-910023-1

Annual Report
Period: 01 October 1987 - 15 July 1988

STUDYING QUANTUM PHASE-BASED ELECTRONIC DEVICES

H. L. Grubin and J. P. Kreskovksy

Scientific Research Associates, Inc.
P.O. Box 1058
Glastonbury, Connecticut 06033-6058

Prepared for

Air Force Office of Scientific Research
Bolling Air Force Base, D.C.

August 1988

STUDYING QUANTUM PHASE-BASED ELECTRONIC DEVICES

ABSTRACT

This report summarizes work performed during the reporting period 01 October 1987 to 15 July 1988 under Contract #F49620-87-C-0055. Work was confined to use of the moments of the density matrix, for examining transport in quantum phase based devices. There are two significant features of the approach: (1) the introduction of Bohm's quantum potential, and (2) the use of moment equations which are self-consistently coupled to Poissons equation. There were a number of significant approximations made during this reporting period that are currently being eliminated: (1) Only two of the minimum of three moment equations have been implemented. (2) Boltzmann statistics was invoked. The results show for a double barrier structure with 500 Angstrom spacer-layers considerable structure in the charge distribution. At low values of bias and corresponding low values of current there is a build up of charge upstream of the first barrier. As well as tunneling into the well. At a critical value of bias a local instability of current occurs and the solutions shows a qualitative difference. Accumulation at the upstream barrier is only marginally altered, and there is a significant charge buildup in the well. The instability appears to be a precursor for this large charge build up. Switching calculations were also performed and indicate switching times of the order of 200 femoseconds.

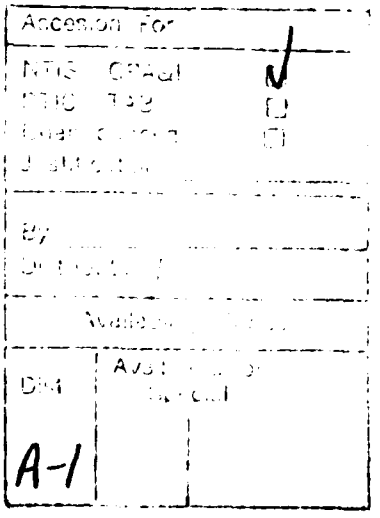

TRANSPORT IN QUANTUM PHASE BASED DEVICES

I. INTRODUCTION

Studies during this first reporting period was confined to Task III of AFOSR Contract #F49620-87-C-0055. This task involves use of the density matrix, and the moments thereof, for examining transport in quantum phase based devices. There are two significant features of the approach taken at Scientific Research Associates, Inc. (SRA):

(1)the introduction of Bohm's quantum potential into the transport formulation, and

(2)the use of moment equations to self-consistently calculate current, all of which are self-consistently coupled to Poissons equation.

Much of the work during this period was devoted to obtaining an understanding of the Bohm quantum potential, which Bohm introduced and used to discuss two-slit interference experiments. In the studies performed at SRA transport was examined in only one dimension. Two dimensional transport is the object of another task. Further there were a number of significant approximations made during this reporting period that are currently being eliminated:
(1) During the present reporting period only two of the minimum of three moment equations have been implemented. The quantum energy balance equation has not been implemented in anything other than its classical form.
(2) Boltzmann statistics was invoked.

II. THE QUANTUM MECHANICAL TRANSPORT EQUATIONS

The transport equations used in the study are obtained under the assumption of a displaced Fermi-Dirac density matrix operator, and include Poisson's equation (expressed in terms of energy):

$$\nabla\epsilon\cdot\nabla E(x) = e^2\Big[\,(n(x,t) - n_o(x)\,\Big] \tag{1}$$

In the above, n is the quantum mechanical ensemble averaged carrier density. The next equation is the zeroth moment or equation of continuity:

$$\frac{\partial n}{\partial t} + \nabla\cdot nv = 0 \tag{2}$$

where nv is the quantum mechanical ensemble averaged current density. The third equation is the momentum balance equation and contains the minimum quantum mechanical description of the problem:

$$\frac{\partial nv}{\partial t} + \nabla\cdot vv = -\frac{n}{m}\nabla(E_c - Q) - \frac{2}{3m}\nabla\left[nk_BT\ G[(E_F-E_c)/k_BT]\right] \tag{3}$$

$$+\left\{\frac{nv\cdot v}{2} + \frac{2nk_BT}{3m}\ G\left[[(E_F-E_c)/k_BT]\right]\frac{\nabla m}{m} + \frac{nv}{\tau_v}\right.$$

where

$$E_c(x,t) = E(x,t) - \chi(x) \tag{4}$$

and $\chi(x)$ is a position dependent electron affinity. There are two important terms in equation (3). The first is the Bohm quantum potential (generalized in include a position dependent effective mass):

$$Q = \frac{\hbar^2}{2n^{1/2}}\frac{\partial}{\partial x}\left(\frac{1}{m(x)}\ \frac{\partial n^{1/2}}{\partial x}\right) \tag{5}$$

The second is the pressure gradient which we have expressed classically. The pressure gradient represents the effect of mixed states. In equation (3) the term $G[(E_F - E_c)/k_BT]$ is given by the ratio of equilibrium Fermi-Dirac integrals:

$$G[(E_F-E_c)/k_BT] = F_{3/2}[(E_F-E_c)/k_BT] \ / \ F_{1/2}[(E_F-E_c)/k_BT] \tag{6}$$

where

$$F_\ell(y) = \frac{2}{\sqrt{\pi}}\int_0^\infty \frac{x^\ell dx}{1+\exp[x-x_F]} \tag{7}$$

is the Fermi-Dirac integral. Figure (1) is a plot of equation (6). Note, in the limit of Boltzmann statistics, where the argument of the function is negative, the function asymptotically approaches 3/2. In the extreme quantum limit where the argument is positive the function asymptotically approaches

$$g[(E_F-E_c)/k_BT] \Rightarrow \frac{3}{5}(E_F-E_c)/k_BT \tag{8}$$

Note, in equilibrium the carrier density is equal to:

$$n = NF_{1/2}[(E_F-E_c)/k_BT] \tag{9}$$

and N is the density of state of electrons:

$$N = \frac{1}{4\pi^3}\left(\frac{2\pi mkT}{\hbar^2}\right)^{3/2} = 2.5\times10^{19}\left(\frac{T}{300}\right)^{3/2}\left(\frac{m}{m_o}\right)^{3/2}\frac{1}{cm^3} \tag{10}$$

and m_o is the free electron mass.

It is worthwhile noting that the use of the above equations does not represent a radical departure from previous quantum mechanical approaches. For example in the limiting situation of a pure state and a position independent effective mass, equation (3) reduces to

$$\frac{\partial nv}{\partial t} + \nabla\cdot nvv = -\frac{n}{m}\nabla(E_c(x)-Q) \tag{11}$$

while the equation of continuity retains its same form. The interpretation is of course, different, with n now representing a probability density. A discussion of equations similar to the above single particle equations is contained in Kramer's **Quantum Mechanics**.

III. DISCUSSION OF THE QUANTUM POTENTIAL

The simplest way to discuss the quantum potential is for steady state and for pure states. In this case equation 9 reduces (in one dimension) to:

$$\frac{\partial}{\partial x}\left[v^2+2(E_c-Q)/m\right] = 0 \tag{12}$$

or

$$v^2 = 2(E-E_c+Q)/m \tag{13}$$

Where E is constant of integration. Now with E_c given by equation 4 a simple barrier, with the vacuum as reference, is shown in figure 2. For $E=-E_o$ where $\chi_2>E_0>\chi_1$, $E-E_c<0$ within the barrier and there is no classical solution. Quantum mechanics teaches, however, that a finite and real (albiet small) current will flow, with carriers tunneling through the barrier. Thus, at the very least, for $v \simeq 0$,

$$Q = E_c-E \tag{14}$$

This situation is illustrated in figure 4, which represent the first of a sequence of calculations performed during the first reporting period. The calculations were performed for the structure shown in figure 3. These calculations were performed using Boltzmann statistics. Additionally in order to reduce the influence of the pressure gradient calculations were performed at 4^oK. The physics at 4^oK is not correctly managed by Boltzmann statistics, and we are currently incorporating Fermi-statistics.

Figure 4 displays the charge density in the structure at a potential of 0.1 volts on the anode boundary. Now in the absence of any barrier and quantum mechanical contributions transport in an $N^{++}N^-$ structure indicates that immediately downstream of the interface there is a region of electron depletion followed by a region where the carrier density asymptotically approaches the background doping level. The same situation occurs when the double barrier is present. But at situations below resonance, where the current level is near zero, there is very little charge in the well. Rather there is strong accumulation of charge at the upstream portion of the first

barrier followed by a rapidly decreasing charge distribution through the first classically forbidden region. A narrow plateau region exists within the well followed by a second rapidly decreasing charge distribution through the second classically forbidden region. It is worthwhile noting that this distribution, with the exception of the first region of charge accumulation is as discussed by Ricco and Azbel.

Figure 4b displays the double barrier within the device, while figure 4c is a sketch of the quantum potential. Of significance here is the fact that the shape of the quantum potential appears to mimic that of the double barrier under applied bias. The value of the quantum potential plus the self-consistent potential much be sufficient large to permit a solution to occur.

IV BIAS DEPENDENT SOLUTIONS

Figure 5 displays the distribution of charge in the device as a function of bias. Note that at low values of bias, between 0.1 and 0.4 the charge distribution inside and outside the well behaves in a qualitatively similar manner. There is a net buildup of charge in the well, and a corresponding increase in the accumulation layer at the upstream portion of the double barrier. At bias levels above 0.5 volts the upstream accumulation layer appears to be unchanged, and increases in bias are accompanied by increases in charge between the N^{++} boundary and the double barrier. The charge in the well, however, continues to increase. Please note that the charge decays through the second barrier at a rate that appears to be independent of bias.

Figure 6 displays the spatial dependence of the self consistent energy and the quantum potential at biases ranging from 0.1 v to 0.8 v. There are several points of note. First, at low values of bias the value of the quantum potential between the barriers nearly tracks the value of the self-consistent energy. At values of potential in excess of 0.4v where there is a qualitative change in the bias dependence of the charge distribution the value of the quantum potential between the barriers is relatively insensitive to changes in bias. At this point we can only speculate as to the origin of this phenomena: The quantum potential involves the ratio of the second derivative of the square root of the charge density to the square root of the charge density. Within the well this appears to be constant. Further, while we have not calculated the zero bias energy level associated with this well, a quick estimate indicates that this value is very near the energy level of the well. More work needs to be done on this point.

There is another point to note. There is structure in the quantum potential upstream of the double barriers. This occurs at the high bias levels and is a consequence of the accumulation of charge upstream of the double barrier structure.

V STRUCTURE OF THE TRANSITION REGION

The transition region occurs at the bias point of 0.5 v, and is accompanied by a current oscillation with a period of approximately 5 fs as seen in figure 7. The oscillation is accompanied by carriers trying to move upstream of the

first barrier. This is illustrated in figure 8, which shows a velocity distribution superimposed upon the energy barriers. Note that at a reference time of 0.0ps the carriers have high velocities upstream of the barrier, within the first barrier, and across the second barrier to the downstream contact. Saturation in the velocity is a consequence of scattering that is included in the calculation. The important point to note here is that at the reference time of 0.8 ps, the carrier velocity in the first barrier has changed sign and locally carriers are moving upstream. Figure 9 shows the corresponding charge distribution as a function of time, over a select region of the device.

Note that for this structure, and in the absence of energy balance and Fermi statistics it was not anticipated that negative conductance would emerge. We are currently incorporating both contributions.

VI. SWITCHING

One calculation was performed to determine the switching time associated with the resonant tunnel structure, subject to the approximations herein. The calculation was performed without inclusion of a position dependent effective mass. (All of the above calculations included a position dependent effective mass). The calculation is displayed in figure 10. It was estimated that a switching time of 250fs occurred.

VII. PERSONNEL

During the course of this study, Dr. Harold L. Grubin. Dr. Marc Cahay, and Mr. John P. Kreskovsky participated in the calculations. In addition, two Associate Research Scientists, Mrs. Beverly Morrison and Mr. George Andrews ran some of the calculations.

VIII. PRESENTATIONS

Discussions of these calculations was presented at the ARO Workshop in Cambridge, Mass. (Fall 87), at the Arizona State University Workshop (Fall 87), at the Radio Science Symposium (University of Colorado (January 88), and at the ETDL Workshop on heterostructure devices (Jan 88).

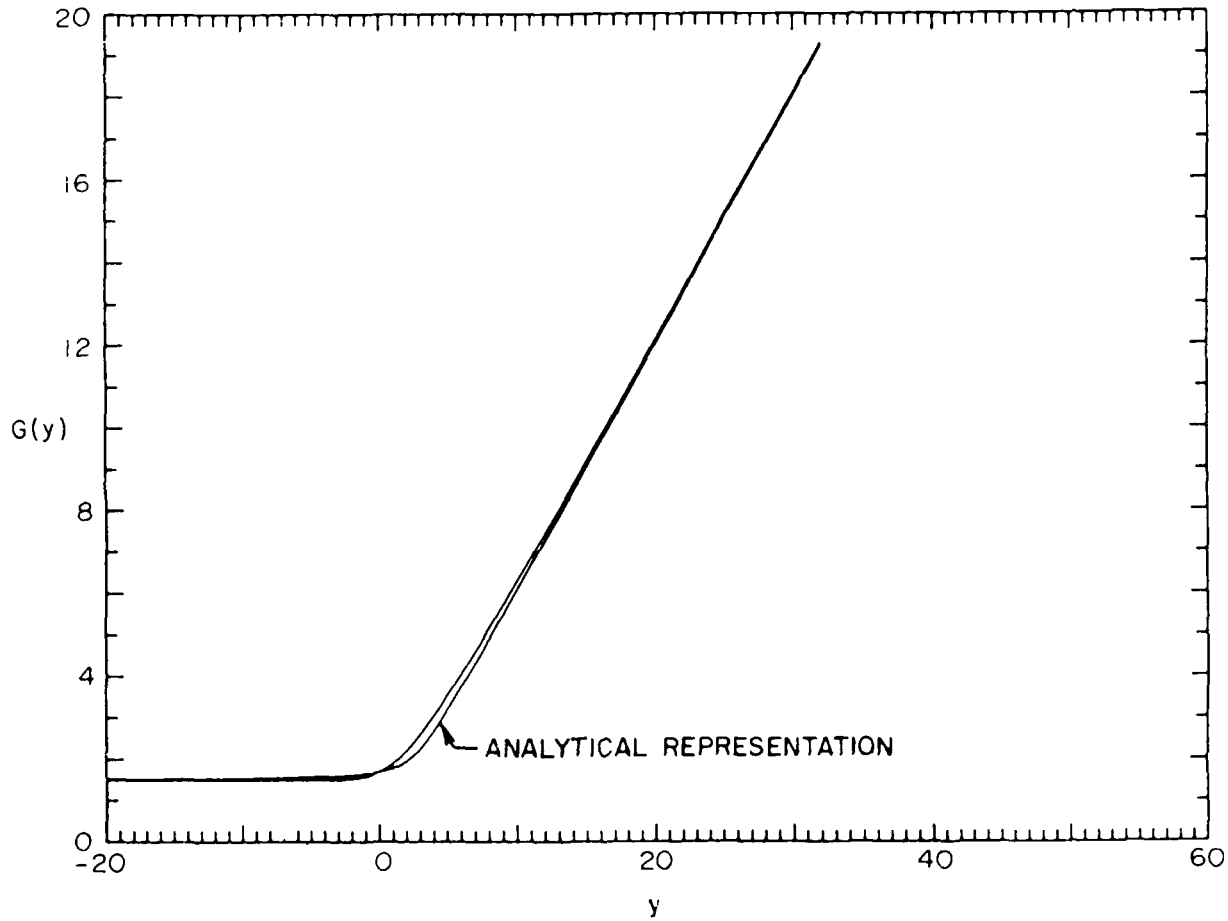

Figure 1. Plot of G(y), given by Equation 6.

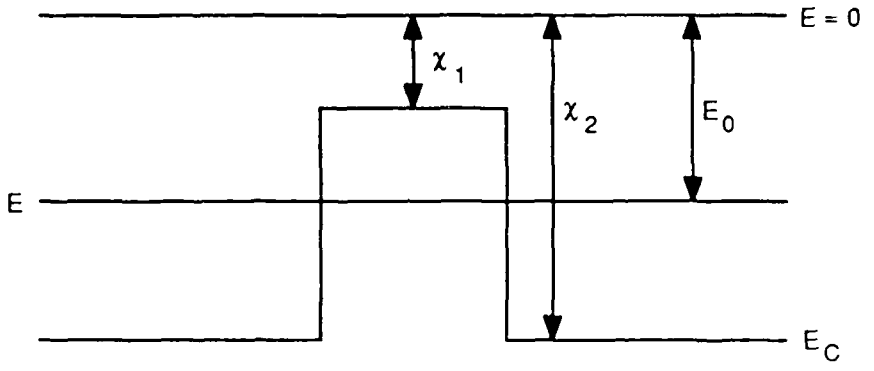

Figure 2. Schematic of a Single Barrier. For $E_0 < \chi_1$, the Barrier is the Chemically Forbidden Region.

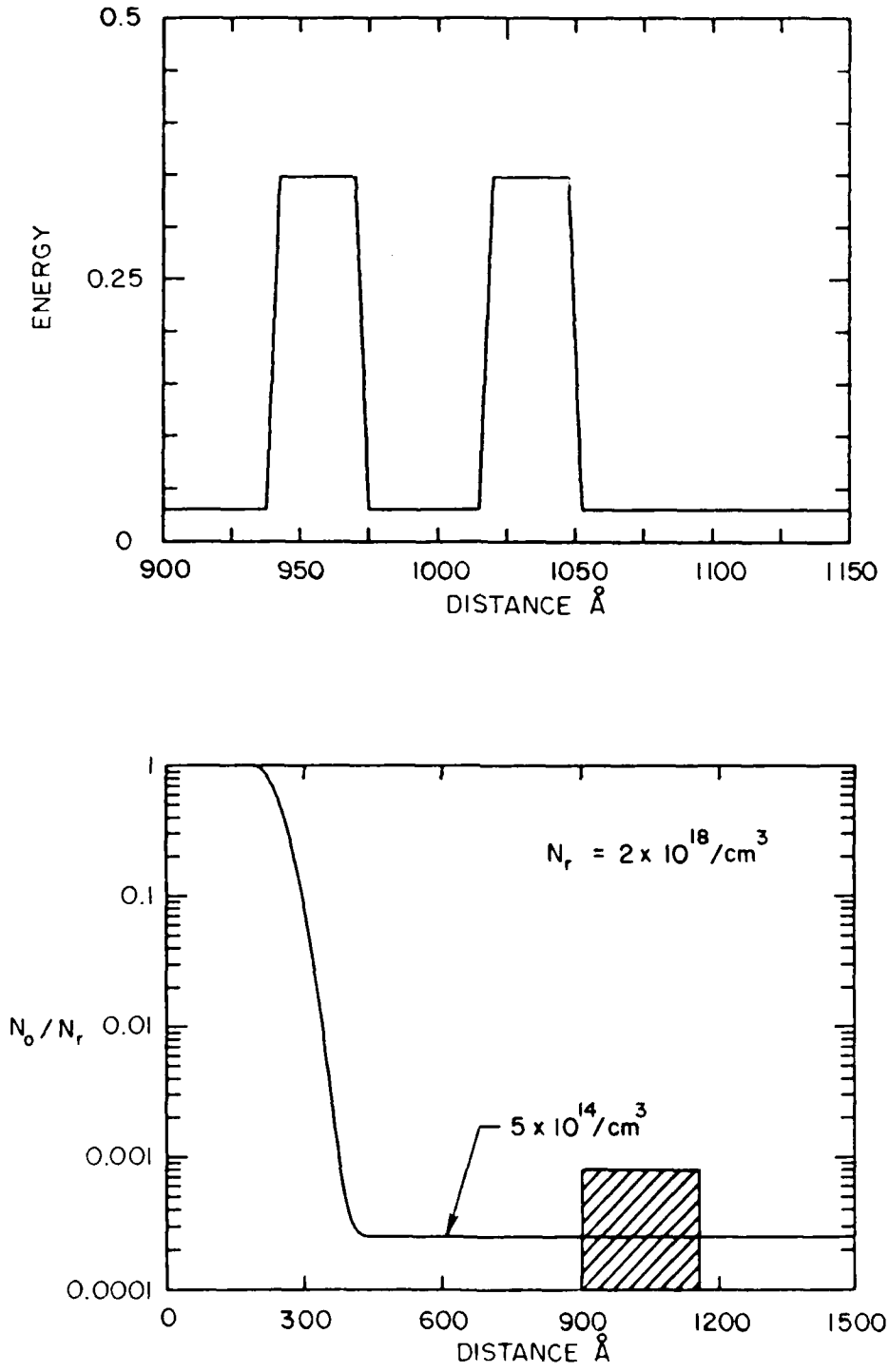

Figure 3. (a) Double Barrier Structure, Axis Coordinates denote Position in Devices.
(b) Doping Profile within Structure. Cross-hatch denotes Figure 3a Region.

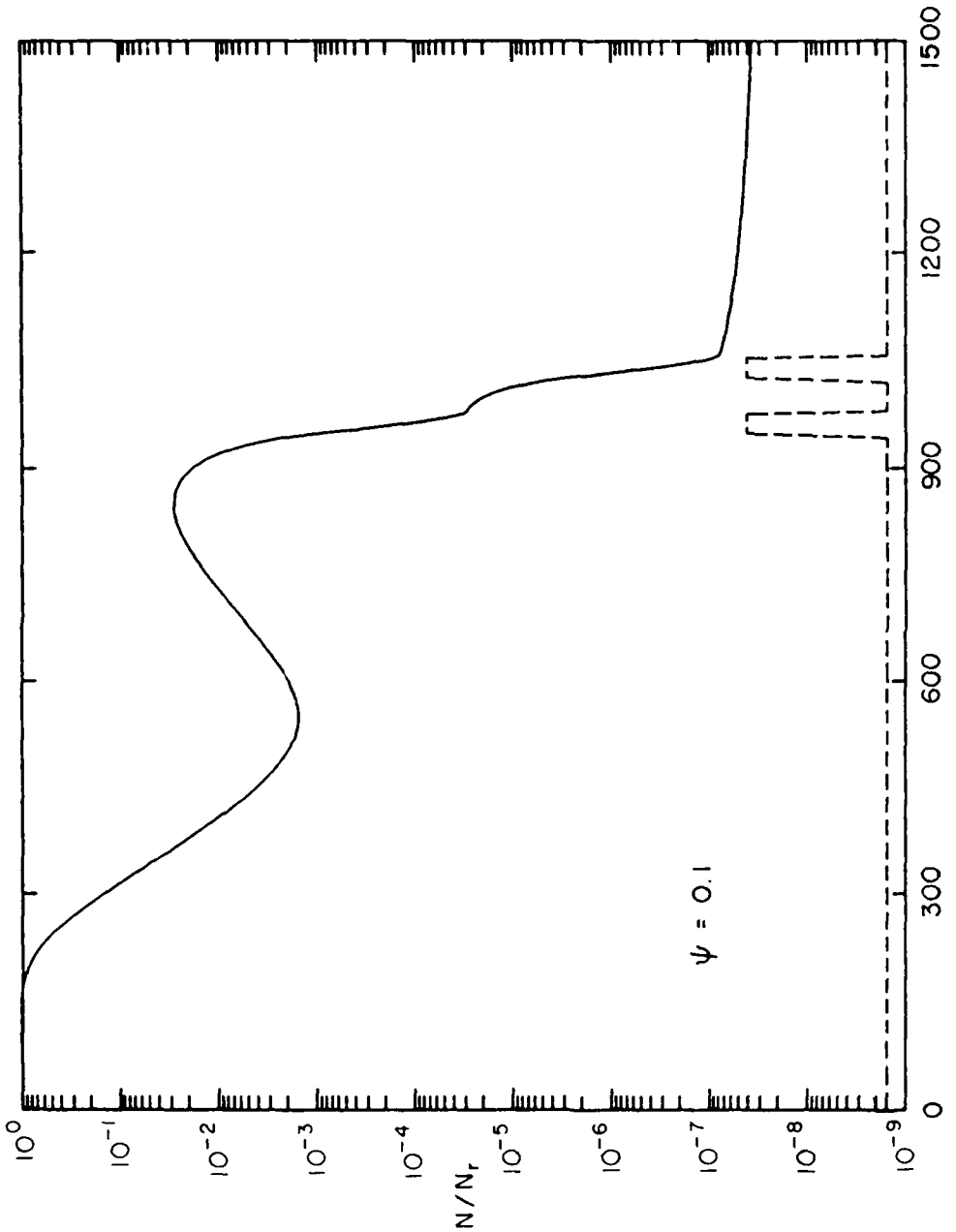

Figure 4a. Distribution of Charge with the Device for y = 0.1.

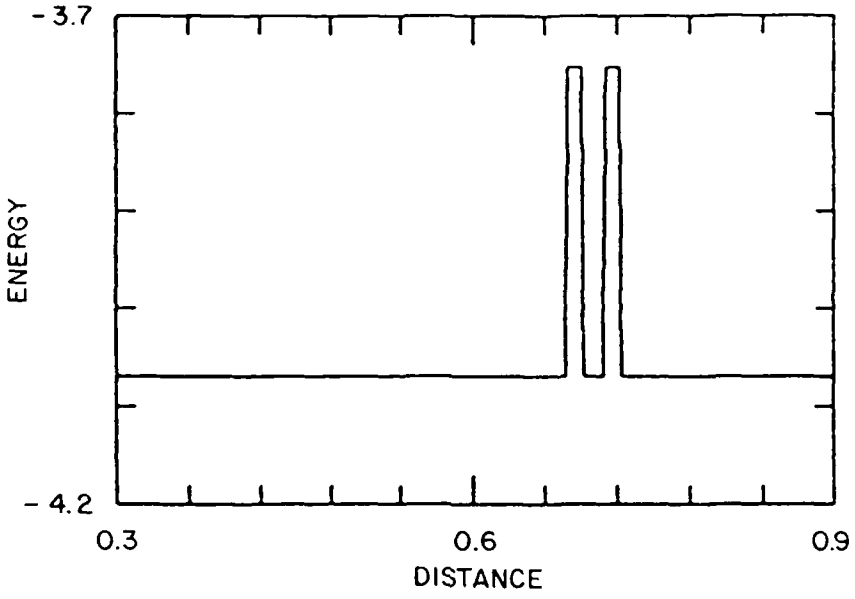

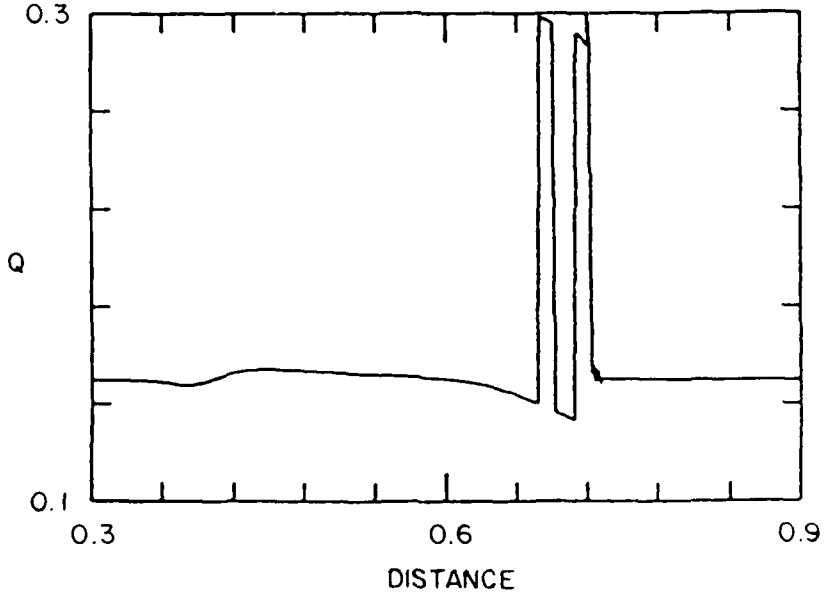

Figure 4b. Double Barrier.

Figure 4c. Quantum Potential.

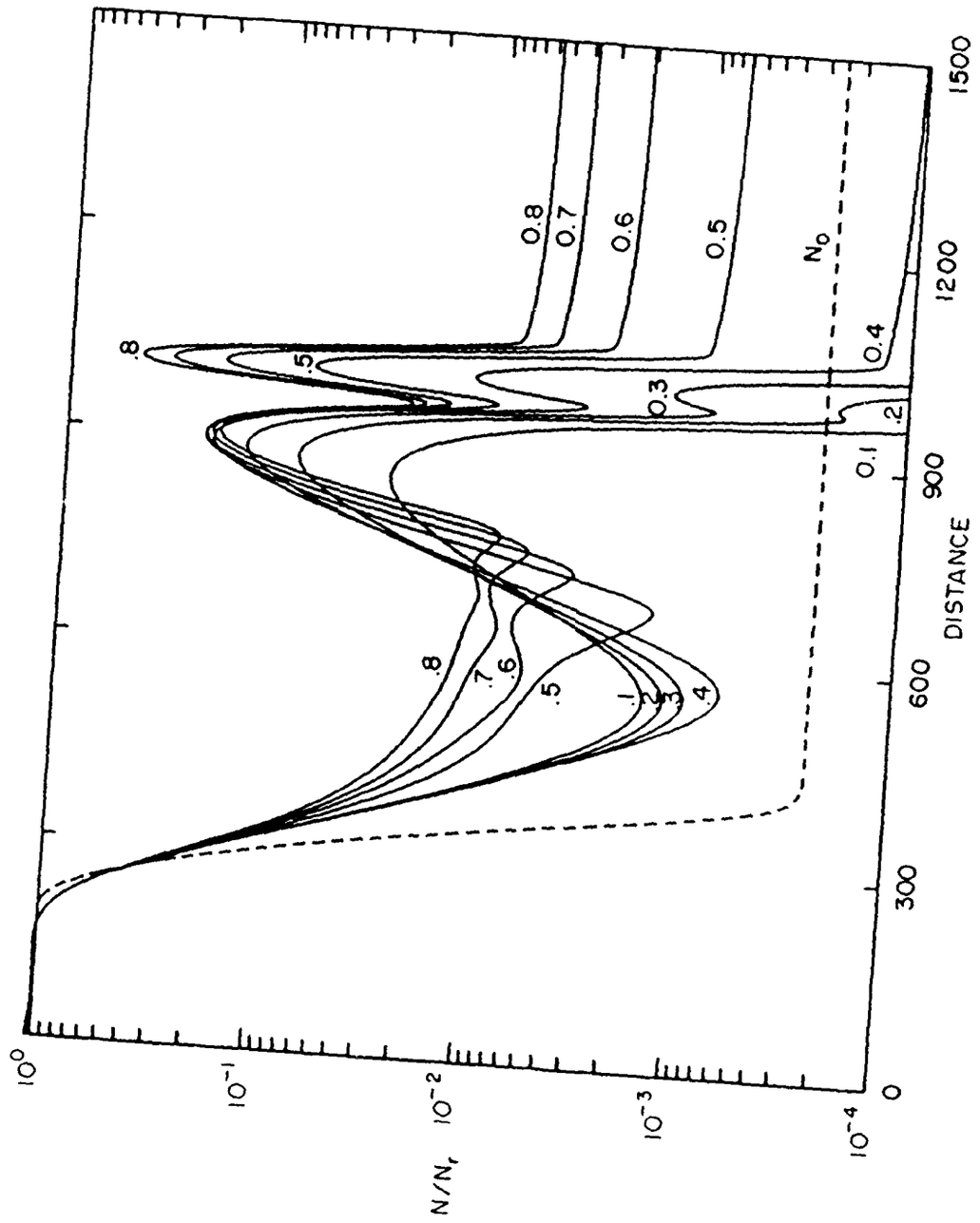

Figure 5. Distribution of Charge with the Device as a Function of Bias.

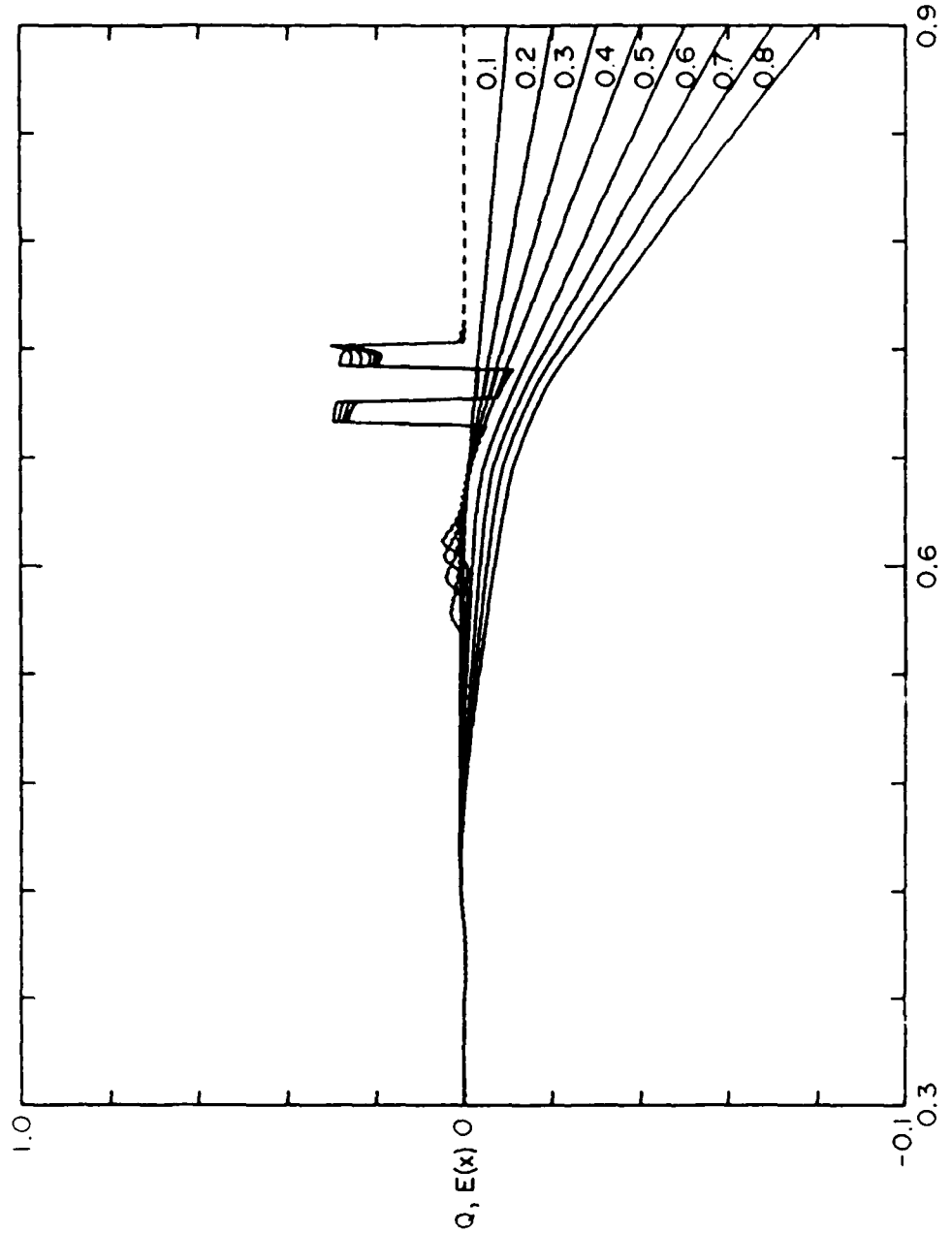

Figure 6. Spatial Dependence of the Self-Consistent Energy and the Quantum Potential.

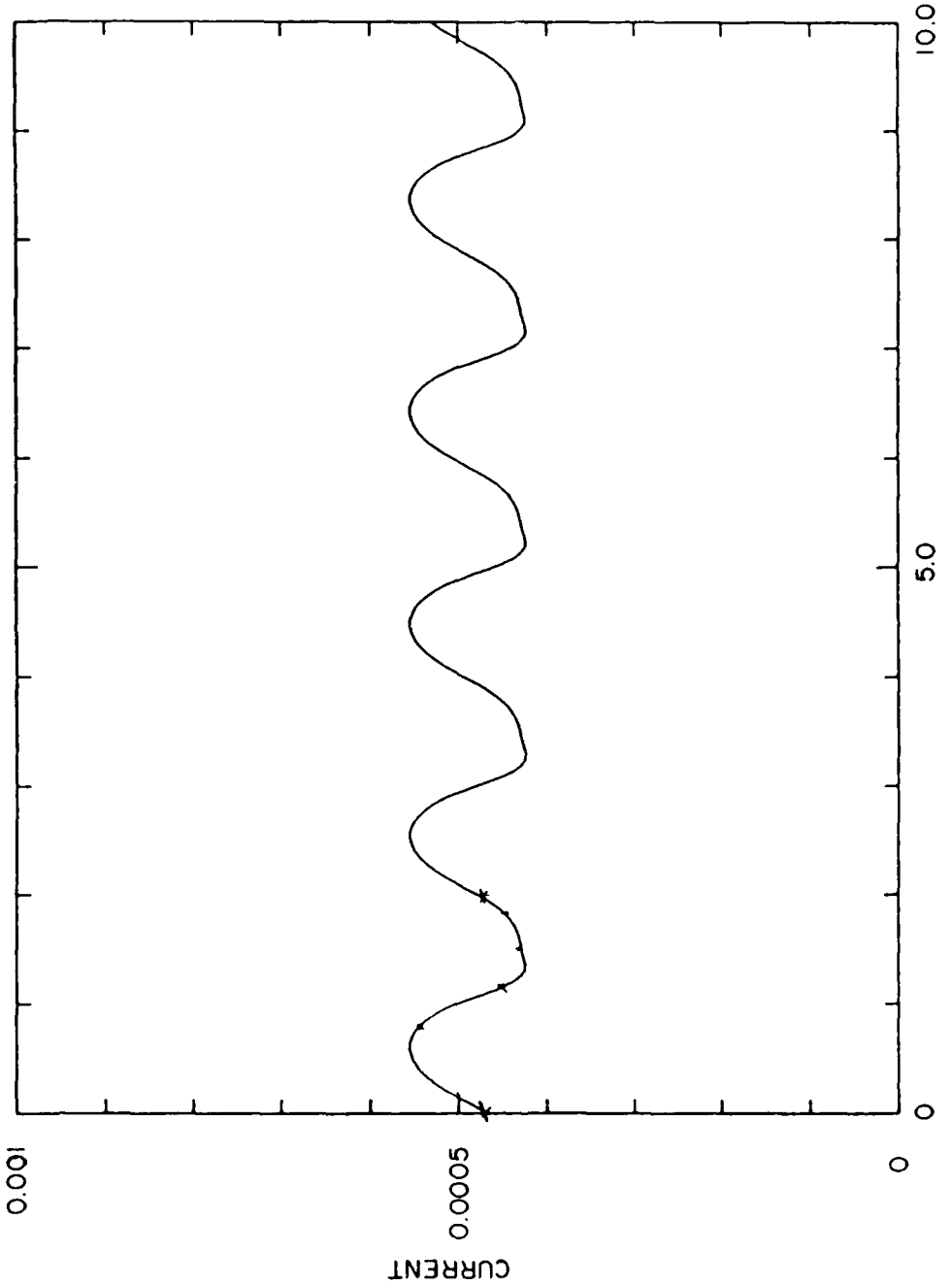

Figure 7. Current Oscillation at the Transition Region.

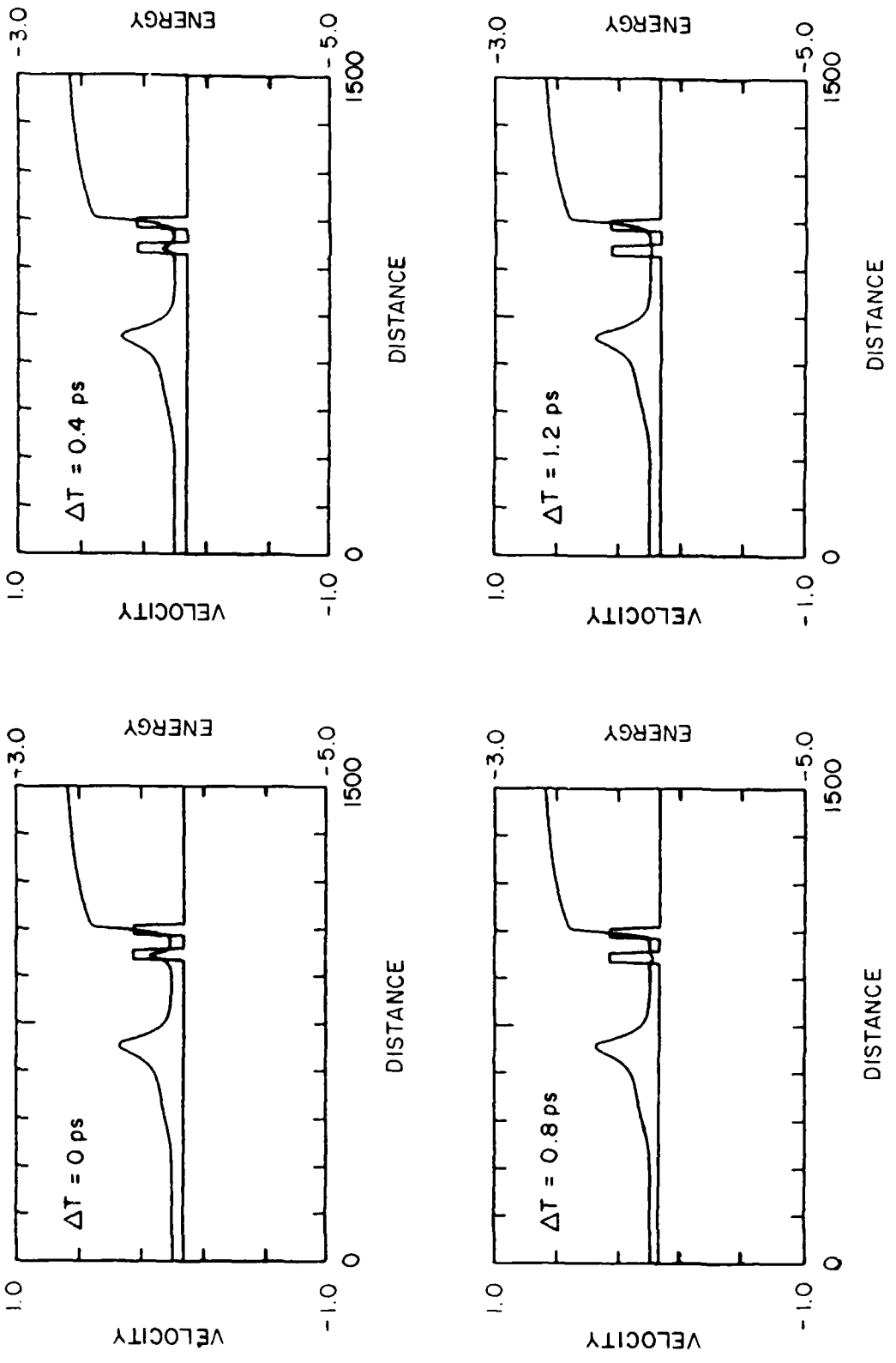

Figure 8. Velocity (in multiples of 10^8 cm/sec) Distribution within the Structure as a Function of Time, for a Bias of 0.5 V.

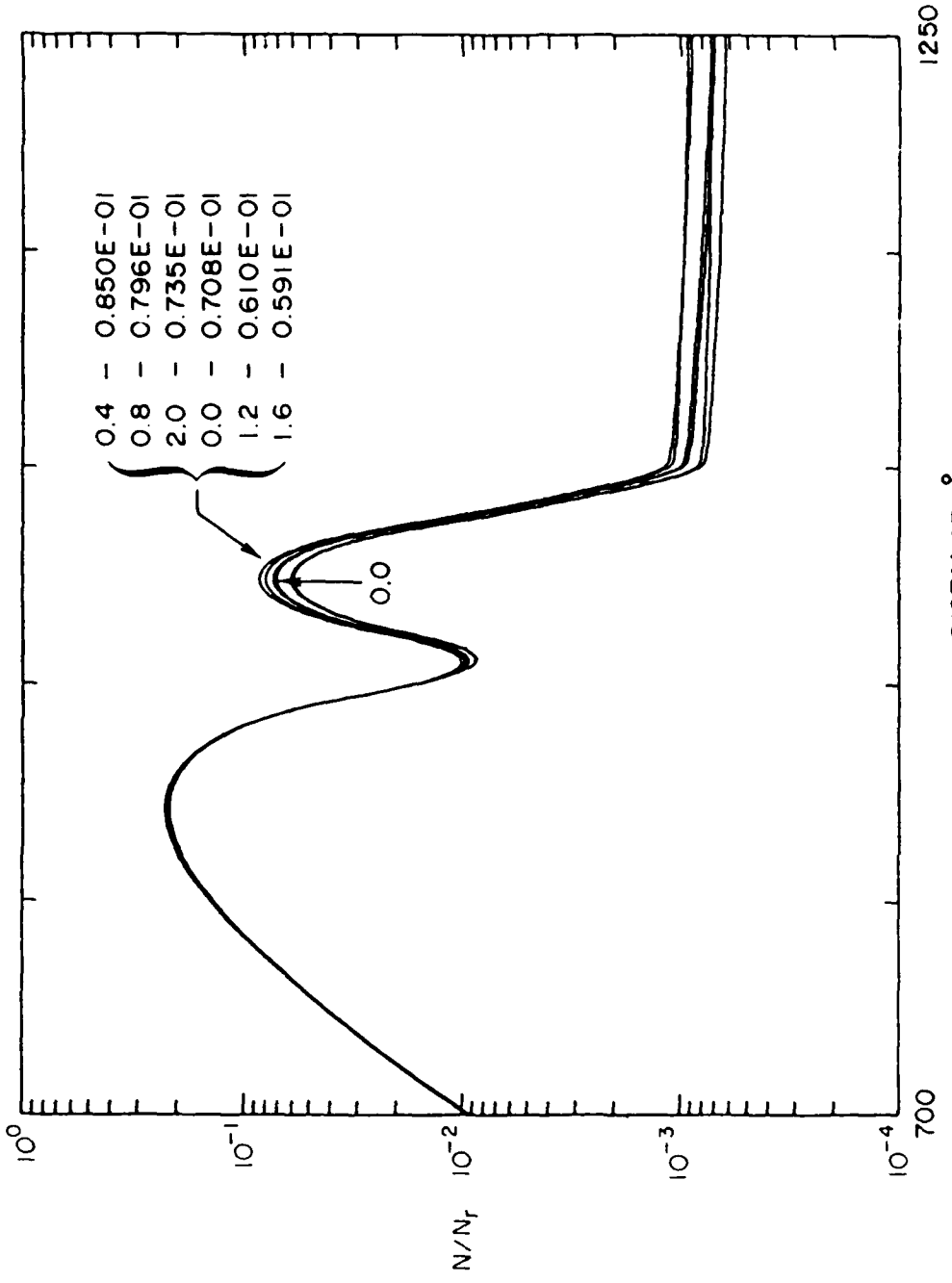

Figure 9. Time Dependent Charge Distribution of a Bias of 0.5 V.

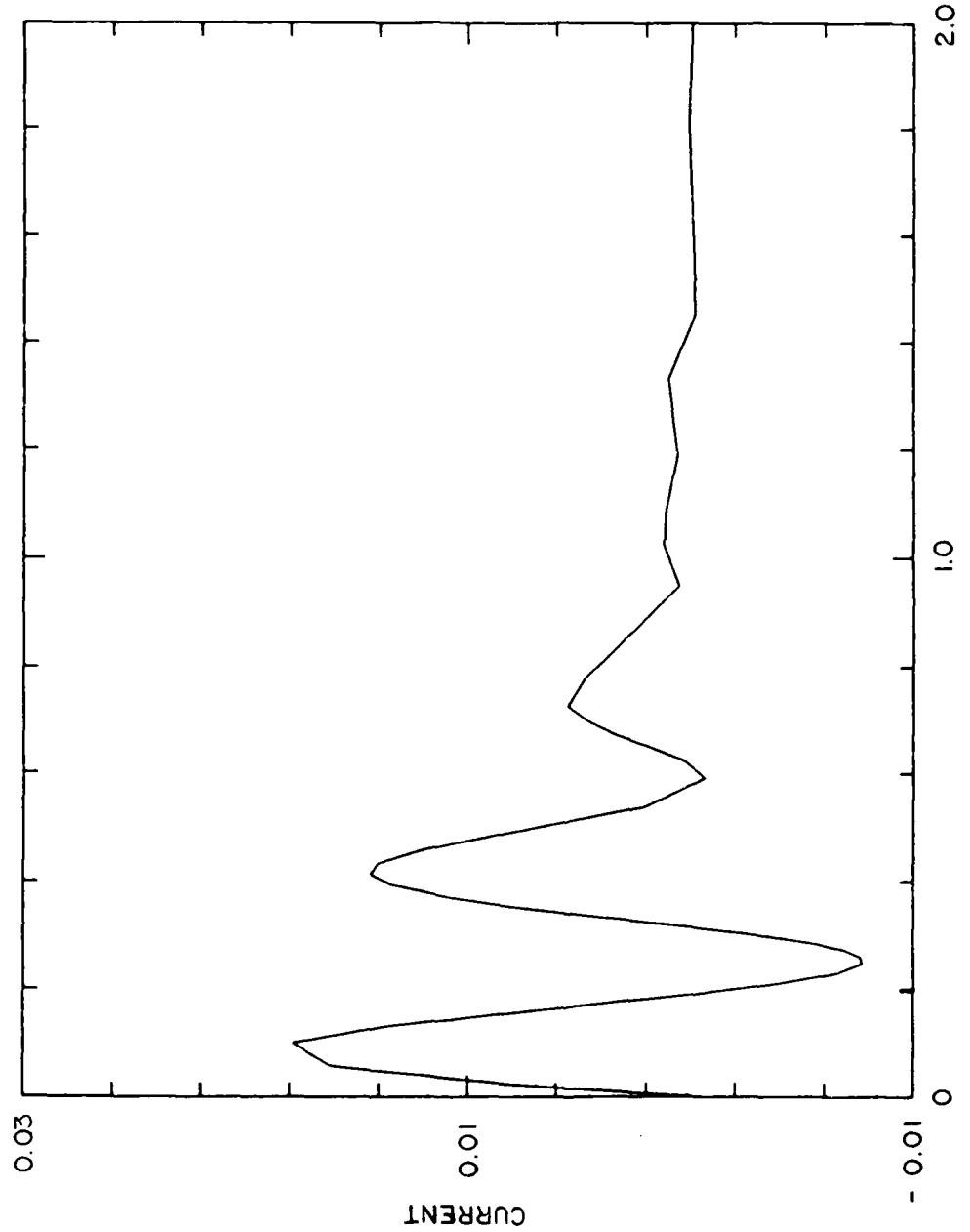

Figure 10. Time Dependent Matching from 0.6 → 0.1 volts.